

Supplementary Information

An A'-A-DA'D-A-A'-typed acceptor enables organic solar cells with high V_{oc} and low nonradiative voltage loss

*Bingjie Zhou^{1,2}, Helin Wang^{*2}, Zehua He^{1,2}, Guoqiang Zheng^{*1}, Ailing Tang², Erjun Zhou^{*1,2}*

¹ College of Materials Science and Engineering, Zhengzhou University, Zhengzhou 450001, China.

² National Center for Nanoscience and Technology, Beijing 100190, China.

E-mail: wanghelin@nanoctr.cn; gqzheng@zzu.edu.cn; zhouej@nanoctr.cn.

Compound 1 (100 mg, 0.094 mmol) and **Compound 2** (120 mg, 0.28 mmol) were dissolved into chloroform (10 mL) and stirred at 65 °C under the protection of nitrogen, pyridine (0.3 mL) was slowly dropped by syringe. The mixture was stirred for 24 hours, then water was added and the mixture was extracted with dichloromethane. The organic phase was dried over anhydrous magnesium sulfate. After removing the solvent, the residue was purified by column chromatography on silica gel employing petroleum ether: dichloromethane (1:1, v/v) as eluent, yielding a black solid **BTA79** (130 mg, 76%). ¹H NMR (400 MHz, CDCl₃) δ 9.15 (s, 2H, Ar), 8.80-8.78 (d, *J* = 8.3 Hz, 2H, Ar), 8.22-8.19 (d, *J* = 13.0 Hz, 4H, Ar), 8.05-8.00 (m, 4H, Ar), 7.75-7.72 (m, 2H, Ar), 4.95-4.90 (q, *J* = 7.3 Hz, 2H, N-CH₂-), 4.79-4.76 (t, *J* = 7.1 Hz, 8H, N-CH₂-), 3.19-3.17 (m, 4H, -CH₂-), 2.16-2.07 (m, 8H, -CH₂-), 1.86-1.82 (t, *J* = 7.3 Hz, 3H, -CH₃), 1.38-1.25 (m, 74H, -CH- or -CH₂-), 0.87-0.82 (m, 24H, -CH₃), 0.77-0.72 (q, *J* = 7.3 Hz, 6H, -CH₃), 0.65-0.60 (q, *J* = 7.1 Hz, 6H, -CH₃). ¹³C NMR (101 MHz, CDCl₃) δ 187.19, 159.77, 151.74, 145.79, 143.89, 143.39, 137.93, 136.79, 135.84, 135.08, 133.06, 132.25, 128.05, 124.87, 120.67, 119.82, 117.99, 115.72, 114.77, 114.26, 110.70, 66.40, 55.95, 54.48, 50.41, 39.31, 38.95, 33.70, 32.58, 32.35, 30.84, 29.05, 28.64, 27.98, 26.55, 25.57, 22.32, 22.01, 21.75, 21.59, 14.45, 13.05, 12.71, 9.34.

Photovoltaic device fabrication

The OSC devices were fabricated with a structure of ITO/PEDOT: PSS/active layer/ PFN-Br/Ag. A 30 nm layer of PEDOT: PSS was spin-casted on pre-cleaned ITO-coated glass at 3000 rpm for 30 s and baked at 150 °C for 15 min before being transferred into the glove box. The Donor: Acceptor/third component (D: A) ratio of 1: 1 (w/w) was dissolved in CF (chloroform) with a total concentration of 15 mg/mL with 0.75% (v/v) CN for 2 hours. Then the active layers were spin-coated from the above solution with thermal annealing of 130°C/10min. A PFN-Br layer was spin-coated on the top of all the active layers at 3000 rpm for 30 s. PFN-Br was dissolved in methanol at a concentration of 0.5 mg/mL. Finally, the Ag (100 nm) metal top

electrode was thermally evaporated onto the active layer under about 4×10^{-4} Pa. The active area of the device was 0.05 cm^2 .

Carrier mobility measurements

The hole mobility of the blend films was measured with the structure of ITO/PEDOT: PSS/active layer /Au and the electron mobility of the blend films was measured with the structure of f ITO/ZnO/active layer/Ag.

The hole and electron mobilities were calculated by the Mott-Gurney equation:

$$J = (9/8)\epsilon_0\epsilon_r\mu(V^2/L^3)$$

Where J stands for current density, ϵ_0 is the permittivity of free space ($8.85 \times 10^{-12} \text{ C} \cdot \text{V}^{-1} \text{ m}^{-1}$), ϵ_r is the relative dielectric constant of the transport medium (assuming that of 3.0), μ is the carrier mobility, V is the internal potential in the device and L is the thickness of the active layer. The active layer thickness is about 100 nm.

Supporting figures and tables

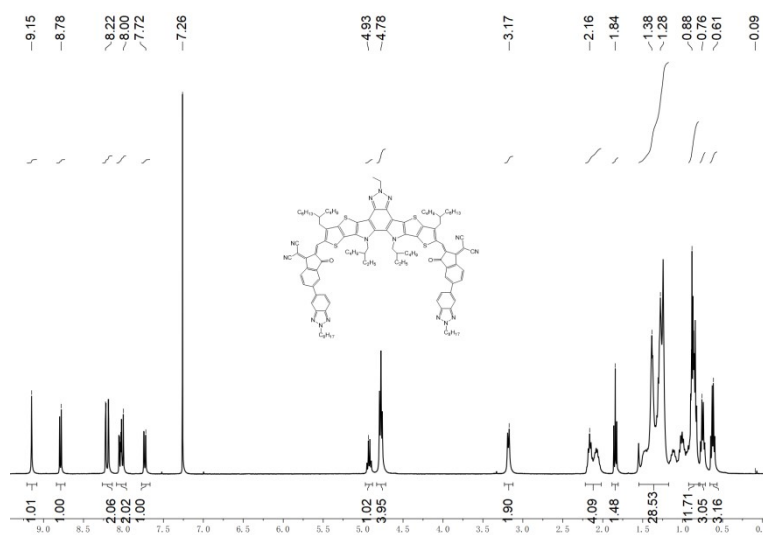


Figure S1. ^1H NMR spectrum of BTA79 in CDCl_3 .

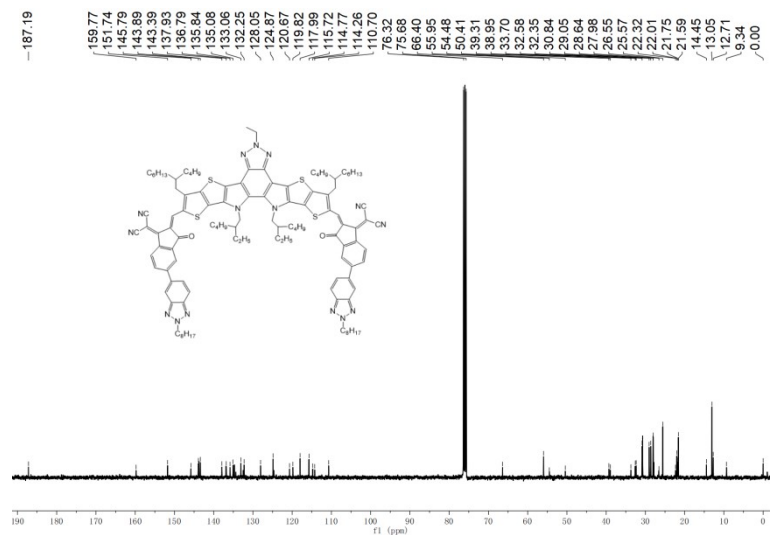


Figure S2. ^{13}C NMR spectrum of **BTA79** in CDCl_3 .

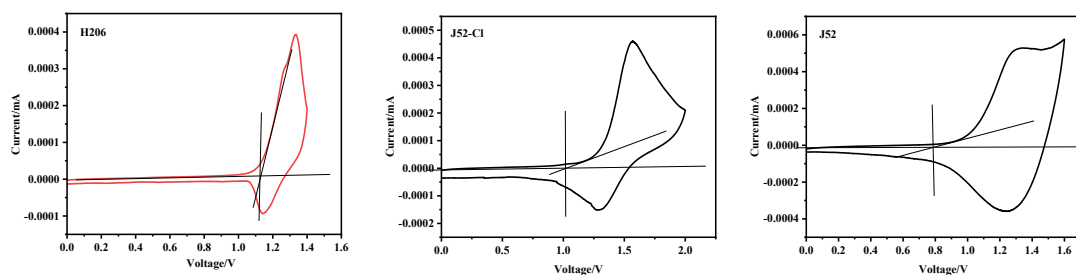


Figure S3. Cyclic voltammograms of **J52**, **J52-Cl**, and **BTA79** with Ag/AgCl as a reference electrode.

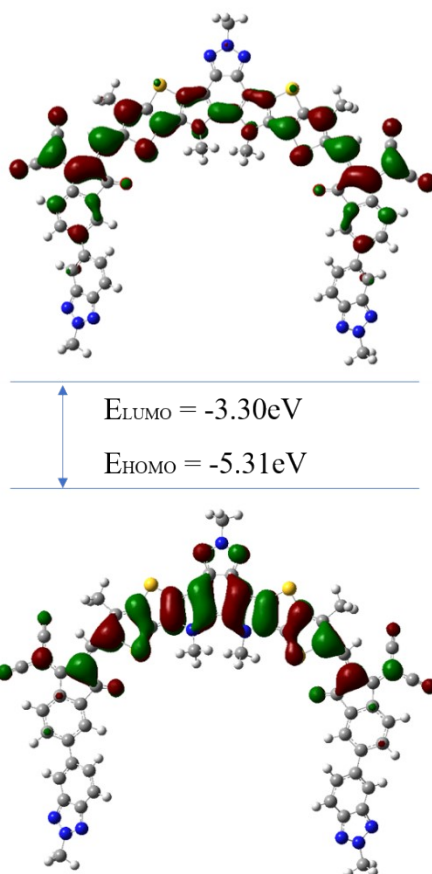


Figure S4. DFT molecular orbital energy levels of BTA79.

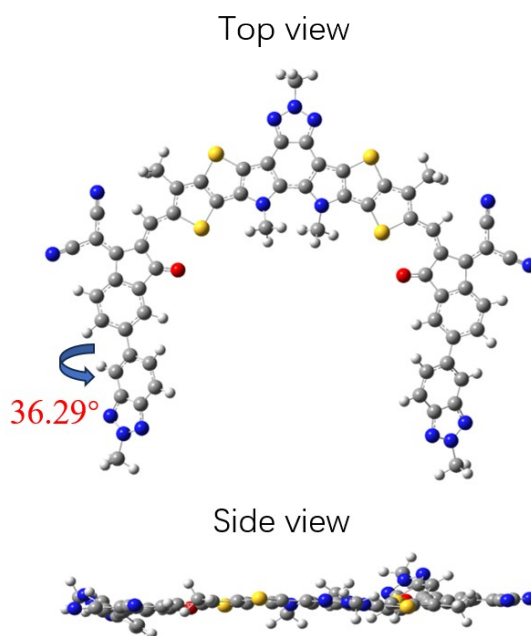


Figure S5. Top view and side view of optimized geometries for BTA79.

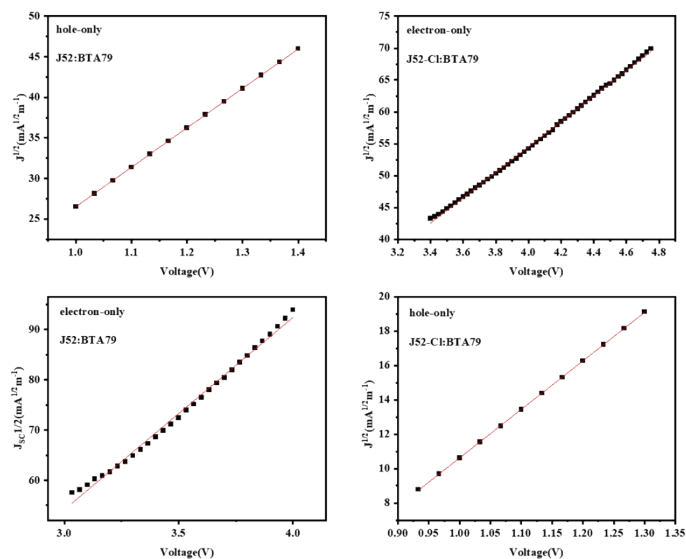


Figure S6. Hole and electron mobility plots from SCLC methods.

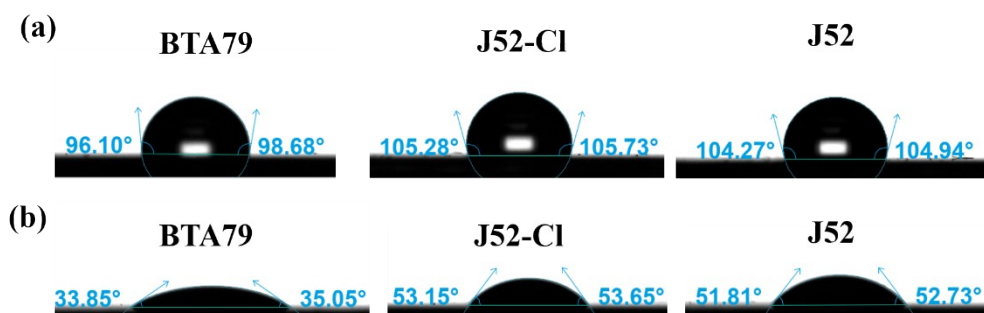


Figure S7. Water (a) and glycerol (b) contact angles for BTA79, J52-Cl, and J52.

Table S1. The optical absorption and electrochemical properties of the related compounds.

Materials	HOMO ^a (eV)	LUMO ^b (eV)	$\lambda_{max, solution}$ (nm)	$\lambda_{max, film}$ (nm)	$\lambda_{onset, film}$ (nm)	$E_{opt} g$ (eV)
J52	-5.13	-3.22	542, 584	548, 594	649	1.91
J52-Cl	-5.39	-3.45	540, 581	544, 589	639	1.94

^a Evaluated by cyclic voltammetry corresponding to their first oxidation potential.

^b deducting the optical bandgap from E_{HOMO} .

Table S2. Summary of device parameters of J52:BTa79 under different conditions.

D: A	Additives	TA (°C)	V_{OC} (V)	J_{SC} (mA cm ⁻²)	FF (%)	PCE (%)
1:1	DPE (0.5%)	/	0.93	14.80	59.02	8.09
	DPE	100	0.93	15.79	59.95	8.78
	DPE	130	0.93	15.97	59.21	8.79
1:1	DIO (0.5%)	/	0.80	4.67	32.25	1.21
	DIO	100	0.93	13.74	59.93	7.60
	DIO	130	0.89	11.32	52.82	5.32
1:1	CN (0.5%)	/	0.92	14.07	55.98	7.26
	CN	100	0.93	16.03	55.74	8.34
	CN	130	0.93	15.81	61.17	8.99
1:1.5	CN (0.5%)	100	0.94	16.86	55.36	8.78
	CN	130	0.93	17.90	56.67	9.48
	CN	160	0.92	17.28	56.22	8.95
1.5:1	CN (0.5%)	100	0.91	16.48	45.90	6.86
	CN	130	0.91	17.17	49.92	7.82
	CN	160	0.88	14.24	13.51	5.43
1:1	CN (0.25%)	130	0.92	19.43	56.09	10.06
	CN (0.5%)	130	0.92	17.52	58.42	9.47
	CN (0.75%)	130	0.93	19.90	57.14	10.11

Table S3. Water and glycerol contact angle for BTA79, J52, and J52-C1.

Surface	BTA79	J52-C1	J52
θ_{Water} (°)	97.39	105.28	104.27
$\theta_{Glycerin}$ (°)	34.45	53.65	52.73
γ (mN m ⁻¹)	43.78	33.06	33.99

References

1. Y. Meng, T. Dai, J. Zhou, H. Wang, A. Tang, Y. Geng and E. Zhou, *ACS Appl. Energy Mater.*, 2023, 6, **19**, 10172-10179.
2. Z. He, T. Dai, M. Ji, A. Tang, H. Wang and E. Zhou, *ACS Macro Lett.*, 2023, 12, **8**, 1144-1150.
3. M. Ichikawa, S. Mochizuki, H. Jeon, S. Hayashi, N. Yokoyama and Y. Taniguchi, *J. Mater. Chem.*, 2011, **21**, 11791-11799.